


## Article

# Estimation of the Soil–Water Characteristic Curve from Index Properties for Sandy Soil in China

Shijun Wang <sup>1</sup>, Xing Guo <sup>1</sup>, Feng You <sup>1</sup>, Zhong Zhang <sup>1</sup>, Tianlun Shen <sup>2</sup>, Yuhui Chen <sup>2</sup> and Qian Zhai <sup>2,\*</sup> <sup>1</sup> Gansu Electric Power Corporation, State Grid Corporation of China, Lanzhou 730050, China<sup>2</sup> School of Civil Engineering, Southeast University, Nanjing 210096, China

\* Correspondence: zhaiqian@seu.edu.cn

**Abstract:** The soil–water characteristic curve (SWCC) is an important parameter of unsaturated soil, and almost all the engineering characteristics of unsaturated soil are more or less related to the SWCC. The SWCC contains important information for geotechnical engineering, water engineering, hydrogeology modelling and climate modelling. It is noted that the experimental measurement of SWCC is costly and time consuming, which limits the implementation of principles of unsaturated soil mechanics in practical engineering. The indirect method, which estimates the SWCC from the index properties of soil, can provide the SWCC with the errors which are within tolerance in practical engineering. In addition, the indirect method can determine SWCC very fast and almost with no cost. In this paper, the domestic sandy soils are selected and the index properties of those sands are used to correlate the SWCC fitting parameters. Consequently, mathematical equations are proposed to estimate SWCC from index properties of domestic sands. The proposed models are trained from 44 sets of experimental data and verified with another independent 8 sets of experimental data from published literature. It is observed that the results from the proposed model agree well with the experimental data from literature.

**Keywords:** soil–water characteristic curve (SWCC); index properties; estimation model; linear regression analysis



**Citation:** Wang, S.; Guo, X.; You, F.; Zhang, Z.; Shen, T.; Chen, Y.; Zhai, Q. Estimation of the Soil–Water Characteristic Curve from Index Properties for Sandy Soil in China. *Water* **2024**, *16*, 2044. <https://doi.org/10.3390/w16142044>

Academic Editor: Jay Jabro

Received: 2 July 2024

Revised: 12 July 2024

Accepted: 18 July 2024

Published: 19 July 2024



**Copyright:** © 2024 by the authors. Licensee MDPI, Basel, Switzerland. This article is an open access article distributed under the terms and conditions of the Creative Commons Attribution (CC BY) license (<https://creativecommons.org/licenses/by/4.0/>).

## 1. Introduction

In conventional geotechnical engineering, engineers only consider the engineering properties of soil. When the problem relates to unsaturated soil, the coupled analysis of geo-environments and unsaturated properties is commonly conducted. In this sustainable coupled analysis, the soil–water characteristic curve (SWCC) is the critical parameter which is commonly adopted as the input information. The SWCC defines the relationship between the water content of soil (expressed as volumetric water content, saturation or gravity water content) and soil suction. Many researchers [1–13] have shown that engineering properties such as pore structure, water retention and its hysteresis, coefficient of permeability and shear strength, tensile strength and modulus could be closely related to the SWCC. On the other hand, the SWCC is also used for the evaluation of water infiltration, slope stability and wetting-induced collapse of loess [14–17]. In practical engineering, different continuous mathematical models have been proposed for the representation of the engineering characteristics of soil. Leong and Rahardjo [18] compared and analyzed various models and experimental results from different types of soil and concluded that Fredlund and Xing's [19] (FX) model had the best performance in the representation of the SWCC for a wide range of soils.

To obtain the SWCC for the whole suction range, a few discrete experimental data points were collected from the laboratory measurements. Subsequently, a continuous mathematical equation was used to best fit with those discrete experimental data and the SWCC curve could be defined by the fitting parameters of the SWCC models. It is noted

that the indoor direct measurement is commonly time consuming and costly, while the indirect method (i.e., estimation from the index properties of soil) is fast and also free. Fredlund and Fredlund [20] revealed that the error associated with the indirect method for the determination of SWCC could satisfy the tolerance requirement in practical engineering. Fredlund et al. [21] categorized the indirect method for the determination of SWCC into four groups: (1) statistical correlation of the water content corresponding to the specific matric suction values; (2) regression model for the fitting parameters of the SWCC model; (3) semi-empirical or physical-empirical model. Recently, the artificial intelligence (AI) technique has provided an alternative method for the estimation of the SWCC [22]. The regression model assumed there was a certain correlation between the fitting parameters of the SWCC model and the index properties of the soil. Liu et al. [23] adopted the effective particle size  $d_{10}$ , non-uniformity coefficient  $C_u$ , porosity  $e$  and other parameters of granular soil to correlate the equivalent capillary height and the fitting parameters  $a$ ,  $m$  and  $n$  in the FX model. Luo et al. [24] showed that the fitting parameters  $a$  and  $n$  in the FX model increased while the parameters  $n$  and  $m$  decreased with an increase in vertical stress and dry density. Chai and Khaimook [25] observed that the fitting parameter  $a$  in the FX model was related to permeability and parameter  $n$  was related to particle size distribution, while parameter  $m$  was related to plasticity index and the content of the fine particles. Both Zapata et al. [26] and Hosseini et al. [27] proposed empirical equations for the estimation of the fitting parameters  $a$ ,  $n$  and  $m$  in the FX model from the weighted plasticity index. Wang et al. [28] proposed a simple equation to estimate the fitting parameter from the dry density. It seems that it is widely recognized that the fitting parameters of the SWCC model can be estimated from the index properties of soil.

As the FX model is commonly considered to be one of the most popular mathematical models for the representation of the SWCC for different types of soil, the fitting parameters in the FX model were estimated from the index properties of the sandy soil in China. Initially, a total of 52 sets of the SWCC experimental data for the sandy soil were collected. Subsequently, the collected data were divided into two groups, one (a total of 44 sets) was used for the training and the other one (a total of 8 sets) was used for the verification. Consequently, new equations were proposed for the estimation of the SWCC for the sandy soil in China from the index properties of soil.

## 2. Methodology

### 2.1. Soil Index Properties Selection

In the FX model, which is illustrated in Equation (1), there was a total of three fitting parameters and one input parameter.

$$\frac{\theta}{\theta_s} = \left[ 1 - \frac{\ln\left(1 + \frac{\psi}{C_r}\right)}{\ln\left(1 + \frac{10^6}{C_r}\right)} \right] \frac{1}{\left\{ \ln\left[e + \left(\frac{\psi}{a}\right)^n\right] \right\}^m} \quad (1)$$

where  $a$ ,  $n$  and  $m$  are the fitting parameters,  $C_r$  is the input parameter, which is a rough estimation of the residual suction (Fredlund and Xing [19] recommended that  $C_r$  be equal to 1500 kPa in most cases),  $\psi$  is the matric suction and  $\theta_s$  is the saturated volumetric water content.

Vanapalli [29] indicated that those fitting parameters can be correlated to the stress history, mineral composition and pore structure. Luo et al. [30] observed that the particle size distribution had a great influence on the SWCC in the low suction region. Aubertin et al. [31] adopted a total of five parameters, such as the effective particle size ( $d_{10}$ ), median particle size ( $d_{30}$ ), limited particle size ( $d_{60}$ ), coefficient of nonuniformity ( $C_u$ ) and the coefficient of the curvature ( $C_c$ ) for the estimation of the SWCC for the sandy soil. Liu and Wen [32] pointed out that parameter  $a$  increased with an increase in the dry density of soil. With the same particle size distribution data (GSD), lower dry density results in the steeper slope of SWCC in the transition curve. As a result, the parameters such as specific gravity

$G_s$ , dry density  $\gamma_d$ ,  $d_{10}$ ,  $d_{30}$ ,  $d_{50}$  and  $d_{60}$ , which were initially used as the input information for the estimation of the fitting parameters of the FX model for the sandy soil in China, were collected. The backward method was adopted to refine the regression equations.

## 2.2. Data Collection

A total of 52 sets of test data covering 19 different sandy soils in China were collected for this paper. Among those sets of data, 44 sets of data, which were randomly selected, were used for the linear regression analysis. The other 8 sets of data were used to verify the reliability of the proposed equation. The index properties of those 52 sets of soil were illustrated in Table 1.

**Table 1.** Index properties of the sandy soil in China.

SN	Soil	Dry Density/ Mg·m <sup>-3</sup>	Specific Gravity/ G <sub>s</sub>	d <sub>60</sub> / mm	d <sub>30</sub> / mm	d <sub>50</sub> / mm	d <sub>10</sub> / mm	References
1	Clay gravel	1.897	2.71	3.547	0.058	2	0.045	Luo et al. [24]
2	Clay gravel	2.065	2.71	3.547	0.058	2	0.045	
3	Clay gravel	2.187	2.71	3.547	0.058	2	0.045	
4	Clay gravel	2.216	2.71	3.547	0.058	2	0.045	
5	Red sandstone soil	1.7	2.7	0.7	0.1	0.5	0.05	Song [33]
6	Red sandstone soil	1.77	2.7	0.7	0.1	0.5	0.05	
7	Red sandstone soil	1.83	2.7	0.7	0.1	0.5	0.05	
8	Red sandstone soil	1.78	2.7	0.7	0.1	0.5	0.05	
9	Red sandstone soil	1.78	2.7	0.7	0.1	0.5	0.05	
10	Red sandstone soil	1.78	2.7	0.7	0.1	0.5	0.05	
11	Mu Wu sand	1.4	2.7	0.28	0.231	0.262	0.188	Zhang [34]
12	Chanhe sand	1.4	2.7	0.513	0.325	0.435	0.238	
13	Riddled sand sand I	1.4	2.7	0.308	0.25	0.289	0.22	
14	Riddled sand sand II	1.4	2.7	0.619	0.502	0.575	0.443	
15	Medium sand	1.75	2.66	0.447	0.3	0.397	0.075	Liu and Wen [32]
16	Medium sand	1.75	2.66	0.447	0.3	0.397	0.075	
17	Medium sand	1.8	2.66	0.447	0.3	0.397	0.075	
18	Fine sand	1.7	2.67	0.349	0.228	0.32	0.061	
19	Fine sand	1.75	2.67	0.349	0.228	0.32	0.061	
20	Fine sand	1.8	2.67	0.349	0.228	0.32	0.061	
21	Silt	1.7	2.68	0.112	0.05	0.093	0.03	
22	Silt	1.75	2.68	0.112	0.05	0.093	0.03	
23	Silt	1.8	2.68	0.112	0.05	0.093	0.03	
24	Sandy soil	1.4	2.7	0.109	0.046	0.087	0.003	He [35]
25	Sandy soil	1.5	2.69	0.109	0.046	0.087	0.003	
26	Sandy soil	1.579	2.7	1.388	0.532	0.895	0.086	Yang et al. [36]
27	Sandy soil	1.38	2.685	0.14	0.096	0.155	0.076	Tian and Kong [37]
28	Sandy soil	1.38	2.69	0.136	0.091	0.149	0.038	
29	Sandy soil	1.38	2.694	0.131	0.086	0.142	0.030	
30	Sandy soil	1.38	2.695	0.127	0.08	0.135	0.026	
31	Sandy soil	1.38	2.683	0.148	0.102	0.16	0.082	
32	Sandy soil	1.38	2.703	0.106	0.038	0.105	0.013	

Table 1. Cont.

SN	Soil	Dry Density/ Mg·m <sup>-3</sup>	Specific Gravity/ G <sub>s</sub>	d <sub>60</sub> / mm	d <sub>30</sub> / mm	d <sub>50</sub> / mm	d <sub>10</sub> / mm	References
33	Hunan sandy soil	1.3	2.7	0.054	0.031	0.047	0.012	Zhu [38]
34	Hunan sandy soil	1.35	2.7	0.054	0.031	0.047	0.012	
35	Hunan sandy soil	1.4	2.7	0.054	0.031	0.047	0.012	
36	Hunan sandy soil	1.45	2.7	0.054	0.031	0.047	0.012	
37	Hunan sandy soil	1.5	2.7	0.054	0.031	0.047	0.012	
38	Hunan sandy soil	1.6	2.7	0.054	0.031	0.047	0.012	
39	Hunan sandy soil	1.6	2.7	0.054	0.031	0.047	0.012	
40	Sandy soil	1.754	2.55	0.375	0.288	0.325	0.238	Zhang [39]
41	Sandy soil	1.888	2.55	0.365	0.273	0.315	0.223	
42	Sandy soil	1.942	2.55	0.35	0.254	0.300	0.204	
43	Sandy soil	2.039	2.55	0.322	0.23	0.272	0.180	
44	Sandy soil	1.996	2.56	0.28	0.235	0.240	0.185	
45	Sandy soil	1.935	2.58	0.32	0.26	0.270	0.210	
46	Sandy soil	1.81	2.59	0.34	0.28	0.290	0.230	
47	Sandy soil	1.683	2.55	0.386	0.304	0.336	0.254	
48	Sandy soil	1.26	2.69	0.136	0.098	0.1	0.079	Tang [40]
49	Sandy soil	1.4	2.53	0.204	0.167	0.193	0.134	Hou [41]
50	Fine sand	1.4	2.55	0.296	0.148	0.237	0.075	Lou [42]
51	Coarse sand	1.4	2.55	0.669	0.34	0.561	0.141	
52	Medium sand	1.4	2.55	0.383	0.196	0.319	0.104	

### 2.3. Data Processing

The fitting parameters ( $a$ ,  $n$  and  $m$ ) in the FX model were determined by best fitting the FX model with the collected experimental data. To avoid invalid samples in the regression, the input parameter  $C_r$  was set at 1500 kPa, and the ranges of the fitting parameters were defined as follows:  $0.01 \leq a \leq 1000$ ,  $0.1 \leq n \leq 20$ ,  $0.1 \leq m \leq 4$  [25]. The determined fitting parameters in the FX model for those 44 sets of sandy soil in China are illustrated in Table 2.

Table 2. The determined fitting parameters in the FX model for the sandy soils.

No.	Soil	FX Model Parameter			R <sup>2</sup>
		A (kPa)	$m$	$n$	
1	Clay gravel	8.835	0.369	1.368	99.88
2	Clay gravel	27.34	0.282	1.663	99.97
3	Clay gravel	27.4	0.11	2.897	99.7
5	Red sandstone soil	39.88	0.515	1.781	99.8
6	Red sandstone soil	64.23	0.7	1.334	99.89
7	Red sandstone soil	72.88	0.67	1.614	99.8
8	Red sandstone soil	61.51	0.48	2.319	99.53
9	Red sandstone soil	47.88	0.768	1.267	98.17
10	Red sandstone soil	155.8	0.53	1.49	99.59
11	Mu Wu sand	2	0.8	5	81.71
12	Chanhe sand	2	0.8	10	87.32
13	Riddled sand sand I	2.288	1.75	13.662	99.39

Table 2. Cont.

No.	Soil	FX Model Parameter			$R^2$
		A (kPa)	$m$	$n$	
16	Medium sand	8.579	0.48	8.641	99.78
17	Medium sand	9.852	0.433	7.368	98.73
18	Fine sand	9.538	0.708	4.281	99.63
19	Fine sand	10.062	0.535	6.405	99.92
21	Silt	17.997	0.771	5.189	99.85
22	Silt	20.138	0.665	4.754	99.73
23	Silt	20.165	0.595	4.382	99.67
24	Sandy soil	3.792	0.645	1.511	99.35
26	Sandy soil	2.600	0.866	4.275	99.86
27	Sandy soil	2.425	0.865	4.332	99.55
28	Sandy soil	3.045	0.726	5.169	99.35
29	Sandy soil	2.305	0.868	2.508	99.84
30	Sandy soil	2.405	0.667	2.716	99.86
32	Sandy soil	2.622	1.483	2.555	99.59
33	Hunan sandy soil	0.734	0.427	1.530	99.87
34	Hunan sandy soil	0.684	0.390	1.415	99.67
35	Hunan sandy soil	0.813	0.399	1.190	99.51
36	Hunan sandy soil	0.971	0.359	1.397	99.64
37	Hunan sandy soil	2.167	0.294	1.920	99.49
39	Hunan sandy soil	3.620	0.258	1.834	99.76
40	Sandy soil	2.119	0.698	15.420	99.56
41	Sandy soil	2.763	0.699	6.164	99.38
42	Sandy soil	13.519	1.195	1.494	99.51
43	Sandy soil	13.519	1.195	1.494	99.59
44	Sandy soil	287.483	3.155	1.029	99.52
45	Sandy soil	75.985	1.514	1.216	99.67
46	Sandy soil	46.452	1.005	1.412	99.94
47	Sandy soil	7.852	0.724	5.576	99.12
48	Sandy soil	0.5	1	2	96.53
49	Sandy soil	10	2	1	94.66
50	Fine sand	8.686	0.759	6.697	99.58
52	Medium sand	7.246	0.882	5.888	99.66

#### 2.4. Statistical Analysis

The multiple linear regression method was used for the mathematical statistical analysis to correlate the fitting parameters in the FX model and the index properties of the soil. In the process of analysis, the backward method was adopted for the refinement of the regression equation. The weakly correlated parameters were discarded based on a significance test. The procedures of the statistical analyses were illustrated as follows:

1. Construct an  $x$ -element regression equation using all  $x$  variables.
2. Calculate the significance test  $p$ -value of these  $x$  independent variables, respectively, and record the maximum value as  $p_j^x = \max\{p_1^x, p_2^x, \dots, p_x^x\}$ .
3. For a given significance level (0.05), it is considered that this variable can be removed from the regression equation if  $p_j^x \geq 0.05$ .

4. Reconstruct the regression equation using the remaining  $x - 1$  variables.
5. Conduct false significance tests for the remaining  $x - 1$  variables, respectively, and mark the maximum value as  $p_j^{x-1} = \max\{p_1^x, p_2^x, \dots, p_{x-1}^x\}$ .
6. If  $p_j^{x-1} \geq 0.05$ , it is considered that the variable can be removed from the regression equation.
7. This cycle ends when the significance  $p$ -value of all independent variables in the regression equation is less than 0.05.

The adjusted coefficient of determination,  $R^2$ , which is defined in Equation (2), was adopted for the evaluation of the performance of the proposed equation.

$$adjusted\ R^2 = 1 - \frac{(1 - R^2)(n - 1)}{(n - x - 1)}, \tag{2}$$

where  $x$  is the number of independent variables and  $n$  is the sample size,  $R$  is the coefficient of the determination.

The results of the multiple linear regression analyses for the correlation of parameters  $a$ ,  $m$  and  $n$  with the index properties of soil were illustrated in Table 3, respectively.

**Table 3.** The results of multiple linear regression analyses for the parameter  $a$ .

Model	Variables	Coefficient	Significance Test $p$ -Value	$R$	$R^2$	Adjusted $R^2$
1	(constant)	-26.252	0.97	0.613	0.376	0.226
	dry density	94.407	0.081			
	specific gravity	-37.974	0.382			
	$d_{60}$	214.464	0.306			
	$d_{30}$	-253.146	0.103			
	$d_{50}$	-224.252	0.469			
2	(constant)	-89.283	0.898	0.602	0.362	0.239
	dry density	97.438	0.068			
	specific gravity	-18.773	0.194			
	$d_{50}$	67.741	0.173			
	$d_{30}$	-236.217	0.219			
3	(constant)	98.38	0.728	0.6	0.355	0.271
	dry density	14.049	0.043			
	specific gravity	-43.285	0.202			
	$d_{50}$	-2.285	0.039			
4	(constant)	-136.225	0.027	0.49	0.24	0.18
	dry density	95.618	0.02			
	$d_{50}$	179.221	0.114			
	$d_{10}$	-20.478	0.258			

Notes: 1. Predictive variables: (constant),  $d_{10}$ ,  $d_{60}$ , dry density, specific gravity,  $d_{30}$ ,  $d_{50}$ ; 2. predictive variables: (constant),  $d_{10}$ , dry density, specific gravity,  $d_{30}$ ,  $d_{50}$ ; 3. predictive variables: (constant),  $d_{10}$ ,  $d_{50}$ , dry density, specific gravity; 4. predictive variables: (constant),  $d_{10}$ ,  $d_{50}$ , dry density.

Table 3 illustrates that the adjusted  $R^2$  for model three was highest (i.e., 0.271), while that of model one was only 0.226. The  $p$ -value of the significance test of each variable in model three was less than 0.05. As a result, model three was selected for the estimation of the fitting parameter  $a$  in the FX model. On the other hand, Tables 4 and 5 show that models six and two give the highest adjusted  $R^2$  for the parameter  $m$  and  $n$ , respectively. Therefore,

model six, as illustrated in Table 4, was adopted for the estimation of the parameter  $m$ , while model two in Table 5 was adopted for the estimation of the parameter  $n$ . Consequently, Equations (3)–(5) were proposed for the estimation of the fitting parameters ( $a$ ,  $n$  and  $m$ ) in the FX model for the sandy soil in China from the index properties as follows:

$$a = 98.38 + 4.287d_{10} + 14.049\gamma_d - 2.285d_{50} - 43.285G_s, \tag{3}$$

$$n = 6.001 - 13.27d_{60} - 3.038\gamma_d + 15.109d_{30} + 18.748d_{50} - 16.111d_{10}, \tag{4}$$

$$m = 0.373 + 3.728d_{10} \tag{5}$$

**Table 4.** The results of multiple linear regression analyses for the parameter  $m$ .

Model	Variables	Coefficient	Significance Test $p$ -Value	$R$	$R^2$	Adjusted $R^2$
1	(constant)	5.345	0.345	0.771	0.594	0.497
	$d_{10}$	5.209	0.018			
	dry density	−0.238	0.568			
	specific gravity	−1.705	0.403			
	$d_{60}$	0.022	0.989			
	$d_{30}$	−0.444	0.712			
2	$d_{50}$	0.158	0.949	0.771	0.594	0.516
	(constant)	5.33	0.328			
	$d_{10}$	5.196	0.007			
	dry density	−0.237	0.555			
	Specific Gravity	−1.701	0.388			
3	$d_{30}$	−0.439	0.696	0.77	0.592	0.532
	$d_{50}$	0.19	0.738			
	(constant)	4.836	0.347			
	$d_{10}$	5.141	0.006			
4	dry density	−0.18	0.614	0.769	0.592	0.548
	specific gravity	−1.541	0.412			
	$d_{30}$	−0.208	0.811			
5	(constant)	4.979	0.321	0.766	0.586	0.558
	$d_{10}$	4.951	0.003			
	dry density	−0.202	0.551			
6	specific gravity	−1.587	0.387	0.758	0.575	0.561
	(constant)	4.652	0.345			
6	$d_{10}$	4.715	0.003	0.758	0.575	0.561
	specific gravity	−1.578	0.385			
6	(constant)	0.373	0.001	0.758	0.575	0.561
	$d_{10}$	3.728	0			

Notes: 1. Predictive variables: (constant),  $d_{50}$ , specific gravity, dry density,  $d_{30}$ ,  $d_{10}$ ,  $d_{60}$ ; 2. predictive variables: (constant),  $d_{50}$ , specific gravity, dry density,  $d_{30}$ ,  $d_{10}$ ; 3. predictive variables: (constant), specific gravity, dry density,  $d_{30}$ ,  $d_{10}$ ; 4. predictive variables: (constant), specific gravity, dry density,  $d_{10}$ ; 5. predictive variables: (constant), specific gravity,  $d_{10}$ ; 6. predictive variables: (constant),  $d_{10}$ .

**Table 5.** The results of multiple linear regression analyses for the parameter  $n$ .

Model	Variables	Coefficient	Significance Test $p$ -Value	$R$	$R^2$	Adjusted $R^2$
1	(constant)	12.504	0.403	0.727	0.528	0.419
	dry density	−3.285	0.02			
	specific gravity	−2.288	0.659			
	$d_{60}$	−12.842	0.025			
	$d_{30}$	14.91	0.001			
	$d_{50}$	18.396	0.03			
	$d_{10}$	−16.552	0.004			
2	(constant)	6.001	0.002	0.724	0.525	0.437
	dry density	−3.038	0.016			
	$d_{60}$	−13.27	0.017			
	$d_{30}$	15.109	0.001			
	$d_{50}$	18.748	0.024			
	$d_{10}$	−16.111	0.004			
	3	(constant)	3.365			
dry density		−0.515	0.732			
$d_{60}$		−0.168	0.653			
$d_{30}$		12.737	0			
$d_{10}$		−15.28	0.005			

Notes: 1. Predictive variables: (constant),  $d_{10}$ ,  $d_{60}$ , dry density, specific gravity,  $d_{30}$ ,  $d_{50}$ ; 2. predictive variables: (constant),  $d_{10}$ ,  $d_{60}$ , dry density,  $d_{30}$ ,  $d_{50}$ ; 3. predictive variables: (constant),  $d_{10}$ ,  $d_{60}$ , dry density,  $d_{30}$ .

### 3. Results and Discussion

The fitting parameters ( $a$ ,  $n$  and  $m$ ) of the remaining eight sets of sandy soil were determined by using Equations (3)–(5) and illustrated in Table 6. The measured experimental data of those remaining eight sets of sandy soil were used to compare with the estimated SWCC by using the fitting parameters in Table 4. The comparisons between the estimated SWCC and measured experimental data were illustrated in Figure 1.

**Table 6.** The estimated fitting parameters ( $a$ ,  $n$  and  $m$ ) in the FX model for the sandy soil in China by using the proposed equation in this paper.

No.	Soil	Linear Regression Model		
		$a$ (kPa)	$m$	$n$
4	Clay gravel	7.833	0.541	0.1
14	Riddled sand sand II	1.764	2.025	4.761
15	Medium sand	6.540	0.653	5.672
20	Fine sand	7.628	0.600	4.363
25	Sandy soil	2.831	0.384	2.277
31	Sandy soil	1.620	0.679	3.064
38	Hunan sandy soil	5.339	0.418	1.268
51	Coarse sand	6.994	0.899	6.253



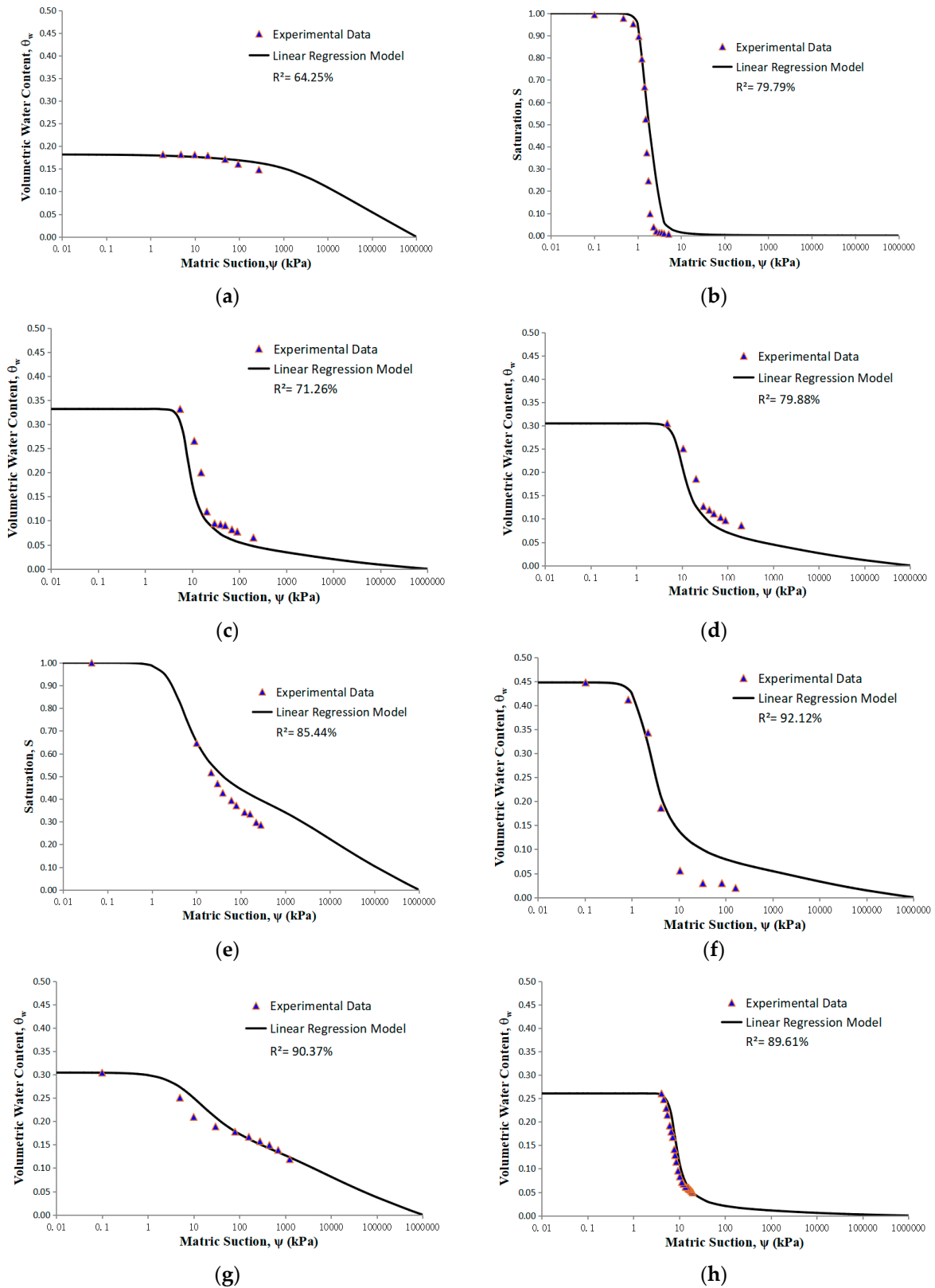


**Figure 1.** Comparison between the predicted and measured SWCCs of the sandy soil in China. (a) Clay gravel; (b) riddled sand sand II; (c) medium sand; (d) fine sand; (e) sandy soil; (f) sandy soil; (g) Hunan sandy soil; (h) coarse sand.

Figure 1 shows that the predicted results are basically consistent with the experimental data, with  $R^2$  mostly greater than 80%. In general, the mathematical model proposed in

this paper predicted the SWCC of sandy soil in China well. As indicated in Figure 1, the estimated SWCC can map the first bending point better than it can the second bending point. The work of Fredlund and Xing [19] indicated that the location of the first bending point was related to the air-entry value, which was related to the large pores in the soil, while the second bending point was related to the residual suction and residual volumetric water content, influenced by the micropores and adsorption action of the soil particles. In this regression analysis, the regression model was proposed for the prediction of the SWCC for sandy soil. In this proposed model, only grain size distribution data (GSD), dry density and specific gravity were adopted as the variables. The effect of the fine contents on the prediction of the SWCC was not considered in the proposed model. Therefore, it seems that more variables such as the percentage of fine contents and the plastic index should be adopted as the variables for the prediction of SWCC for the soil with high fine contents.

#### 4. Conclusions and Recommendations

1. The linear regression analyses were conducted to investigate the correlations between the fitting parameters in the FX model and the index properties of sandy soil in China. A total of 52 sets of experimental data were collected in this paper, 42 sets of data were used to train the correlation equations, while the other 8 sets of data were used for the verification of the proposed equation. It was observed that the proposed equation could predict the SWCC of sandy soil in China well.
2. As only limited data for both the drying and the wetting SWCCs can be collected from the literature, only the dry SWCC data are used for the regression analyses. The hysteresis of the SWCC was not considered in this paper. More research is required on the estimation of the wetting SWCC.
3. It is known that the SWCC of the coarse-grained soil is mainly affected by the grain size distribution data (GSD) and packing density. In the proposed model, only GSD, dry density and specific gravity were used as variables to train the prediction model, and the effects of the fine contents and the plastic index on the SWCC were not considered. Therefore, it was observed that the proposed equation can perform well for soil with low fine contents, and perform less accurately for soil with high fine contents.

**Author Contributions:** Conceptualization, S.W.; methodology, S.W.; formal analysis, X.G.; investigation, F.Y.; data curation, Y.C. and Z.Z.; writing—original draft preparation, S.W., Y.C., Q.Z. and T.S.; writing—review and editing, T.S. and F.Y.; supervision, Q.Z. All authors have read and agreed to the published version of the manuscript.

**Funding:** This research received no external funding.

**Data Availability Statement:** Data are contained within the article.

**Conflicts of Interest:** The authors declare no conflicts of interest.

#### References

1. Zhai, Q.; Rahardjo, H. Estimation of permeability function from the soil–water characteristic curve. *Eng. Geol.* **2015**, *199*, 148–156. [[CrossRef](#)]
2. Zhai, Q.; Rahardjo, H.; Satyanaga, A. Estimation of unsaturated shear strength from soil–water characteristic curve. *Acta Geotech.* **2019**, *14*, 1977–1990. [[CrossRef](#)]
3. Rahimi, A.; Rahardjo, H.; Leong, E.C. Effect of range of soil–water characteristic curve measurements on estimation of permeability function. *Eng. Geol.* **2015**, *185*, 96–104. [[CrossRef](#)]
4. Rahimi, A.; Rahardjo, H.; Leong, E.C. Effects of soil–water characteristic curve and relative permeability equations on estimation of unsaturated permeability function. *Soils Found.* **2015**, *55*, 1400–1411. [[CrossRef](#)]
5. Sarker, D.; Wang, J.X. Experimental study on soil–water retention properties of compacted expansive clay. In *Advances in Transportation Geotechnics IV: Proceedings of the 4th International Conference on Transportation Geotechnics*; Tutumluer, E., Nazarian, S., Al-Qadi, I., Qamhia, I.I., Eds.; Springer International Publishing: Cham, Switzerland, 2022; Volume 3, pp. 433–445.
6. Zhai, Q.; Rahardjo, H.; Satyanaga, A.; Dai, G.L. Estimation of tensile strength of sandy soil from soil–water characteristic curve. *Acta Geotech.* **2020**, *15*, 3371–3381. [[CrossRef](#)]

7. Zhai, Q.; Zhang, R.Z.; Rahardjo, H.; Satyanaga, A.; Dai, G.L.; Gong, W.M.; Zhao, X.L.; Chua, Y.S. A new mathematical model for the estimation of shear modulus for unsaturated compacted soils. *Can. Geotech. J.* **2024**, *in press*. [[CrossRef](#)]
8. Qin, W.J.; Fan, G.S.; Li, H.X. Estimation and predicting of soil water characteristic curve using the support vector machine method. *Earth Sci. Inform.* **2023**, *16*, 1061–1072. [[CrossRef](#)]
9. Peranić, J.; Prodan, M.V.; Škuflić, R.; Arbanas, Z. Preliminary Experiences in Determining the Soil–Water Characteristic Curve of a Sandy Soil Using Physical Slope Modeling. *Water* **2024**, *16*, 1859. [[CrossRef](#)]
10. Wen, T.D.; Wang, P.P.; Shao, L.T.; Guo, X.X. Experimental investigations of soil shrinkage characteristics and their effects on the soil water characteristic curve. *Eng. Geol.* **2021**, *284*, 106035. [[CrossRef](#)]
11. Wen, T.D.; Shao, L.T.; Guo, X.X.; Zhao, Y.R. Experimental investigations of the soil water retention curve under multiple drying–wetting cycles. *Acta Geotech.* **2020**, *15*, 3321–3326. [[CrossRef](#)]
12. Wen, T.D.; Chen, X.S.; Luo, Y.W.; Shao, L.T.; Niu, G. Three-dimensional pore structure characteristics of granite residual soil and their relationship with hydraulic properties under different particle gradation by X-ray computed tomography. *J. Hydrol.* **2023**, *618*, 129230. [[CrossRef](#)]
13. Wen, T.D.; Chen, X.S.; Shao, L.T. Effect of multiple wetting and drying cycles on the macropore structure of granite residual soil. *J. Hydrol.* **2022**, *614*, 128583. [[CrossRef](#)]
14. Jiang, T.; Zhao, J.D.; Zhang, J.R.; Wang, L.J.; Song, C.Y.; Zhai, T.Y. Hydromechanical behavior and prediction of unsaturated loess over a wide suction range. *Geomech. Eng.* **2021**, *26*, 275–288.
15. Meskini-Wishkaee, F.; Mohammadi, M.H.; Vanclooster, M. Predicting the soil moisture retention curve from soil particle size distribution and bulk density data using a packing density scaling factor. *Hydrol. Earth Syst. Sci.* **2014**, *18*, 4053–4063. [[CrossRef](#)]
16. Torabi, M.; Sarkardeh, H.; Mirhosseini, S.M.; Samadi, M. Effect of water temperature and soil type on infiltration. *Geomech. Eng.* **2023**, *32*, 445–452.
17. Zhai, Q.; Tian, G.; Ye, W.M.; Rahardjo, H.; Dai, G.L.; Wang, S.J. Evaluation of unsaturated soil slope stability by incorporating soil water characteristic curve. *Geomech. Eng.* **2022**, *28*, 637–644.
18. Leong, E.C.; Rahardjo, H. Review of soil-water characteristic curve equations. *J. Geotech. Geoenviron. Eng.* **1997**, *12*, 1106–1117. [[CrossRef](#)]
19. Fredlund, D.G.; Xing, A. Equations for the soil-water characteristic curve. *Can. Geotech. J.* **1994**, *31*, 521–532. [[CrossRef](#)]
20. Fredlund, D.G.; Fredlund, M.D. Application of ‘Estimation Procedures’ in Unsaturated Soil Mechanics. *Geosciences* **2020**, *10*, 364. [[CrossRef](#)]
21. Fredlund, M.D.; Wilson, G.; Fredlund, D.G. Use of the grain-size distribution for estimation of the soil-water characteristic curve. *Can. Geotech. J.* **2002**, *39*, 1103–1117. [[CrossRef](#)]
22. Li, Y.; Vanapalli, S.K. Prediction of soil-water characteristic curves using two artificial intelligence (AI) models and AI aid design method for sands. *Can. Geotech. J.* **2022**, *59*, 129–143. [[CrossRef](#)]
23. Liu, Y.; Wei, C.F.; Fang, Q. Implicit integration algorithm of a hydro-mechanical coupling constitutive model for unsaturated soils. *Rock Soil Mech.* **2014**, *35*, 365–370.
24. Luo, Q.X.; Huang, J.; Chen, Q. Influence of vertical stress and dry density on soil-water characteristic curve of gravelly soil. *Rock Soil Mech.* **2014**, *35*, 729–734+743.
25. Chai, J.; Khaimook, P. Prediction of soil-water characteristic curves using basic soil properties. *Transp. Geotech.* **2020**, *22*, 100295. [[CrossRef](#)]
26. Zapata, C.E.; Houston, W.N.; Houston, S.L.; Walsh, K.D. Soil-water characteristic curve variability. In *Advances in Unsaturated Geotechnics*; American Society of Civil Engineers: Reston, VA, USA, 2000; pp. 84–124.
27. Mir Mohammad Hosseini, S.M.; Ganjian, N.; Pashang Pisheh, Y. Estimation of the water retention curve for unsaturated clay. *Can. J. Soil. Sci.* **2011**, *91*, 543–549. [[CrossRef](#)]
28. Wang, Y.; Li, T.L.; Li, P.; Lei, Y.L.; David, D. Lawrence. Measurement and Uniform Formulation of Soil-Water Characteristic Curve for Compacted Loess Soil with Different Dry Densities. *J. Adv. Civ. Eng.* **2021**, *2021*, 6689680.
29. Vanapalli, S.K.; Fredlund, D.G.; Pufahl, D.E. The influence of soil structure and stress history on the soil-water characteristics of a compacted till. *Geotechnique* **1999**, *49*, 143–159. [[CrossRef](#)]
30. Luo, X.Y.; Liu, W.P.; Fu, M.F. Effects of gradation and vertical stress on soil-water characteristic curve in collapsing erosion area. *J. Southeast Univ. (Nat. Sci. Ed.)* **2016**, *46* (Suppl. S1), 235–240.
31. Aubertin, M.; Mbonimpa, M.; Bussiere, B.; Chapuis, R.P. A model to predict the water retention curve from basic geotechnical properties. *Can. Geotech. J.* **2003**, *40*, 1104–1122. [[CrossRef](#)]
32. Liu, J.J.; Wen, S.J. Effect of Dry Density and Particle Size on Soil-water Characteristic Curve of Unsaturated Tailing Sand. *Chin. J. Undergr. Space Eng.* **2021**, *17*, 1437–1443.
33. Song, L.L. *A Study of the Red Sandstone Soil Slope Stability under Rainfall Condition*; Jiangxi University of Science and Technology: Ganzhou, China, 2018.
34. Zhang, S.; Cheng, J.X.; Liu, F.Y. Pedotransfer functions to describe water retention and unsaturated strength behaviors of sandy soils based on particle size parameters. *J. Hydraul. Eng.* **2020**, *51*, 479–491.
35. He, J.T. *The Factors Affecting the Soil-Water Characteristic Curve and Its Prediction*; Guilin University of Technology: Guilin, China, 2017.

36. Yang, M.H.; Wang, W.Y.; Deng, B. The shearing capacity of the interface between unsaturated sandy soil and the concrete surface. *J. Railw. Sci. Eng.* **2022**, *19*, 409–418.
37. Tian, H.N.; Kong, L.W. Experimental study of the effect of the fine contents on the soil water characteristic curve of the sandy soil. *Rock Soil Mech.* **2010**, *31*, 56–60.
38. Zhu, X.L. *A Study of the Pattern of the Particles and Its Effect on the Soil Water Retention Characteristic*; Hubei University of Technology: Wuhan, China, 2019.
39. Zhang, L.Q. *The effect of the Fine Contents and the Degree of Saturation on the Shear Characteristic of Unsaturated Soil*; Beijing Jiaotong University: Beijing, China, 2020.
40. Tang, X.Y. *The Macro-Micro Study of the Soil-Water Characteristic Curve of Sandy Soil in Nanjing*; Nanjing University: Nanjing, China, 2017.
41. Hou, S.Y. *The Seepage Experimental Study of Unsaturated Silty and Sandy Soil and Its Application in the Dual Capillary Barrier System*; China University of Geosciences (Wuhan): Wuhan, China, 2018.
42. Lou, A.Y. *A Study of the Soil Water Retention Curve of Sandy Soil under Frozen and Thaw Condition and Its Sensitivity*; Heilongjiang University: Harbin, China, 2021.

**Disclaimer/Publisher’s Note:** The statements, opinions and data contained in all publications are solely those of the individual author(s) and contributor(s) and not of MDPI and/or the editor(s). MDPI and/or the editor(s) disclaim responsibility for any injury to people or property resulting from any ideas, methods, instructions or products referred to in the content.